

Simple observables from fat link fermion actions

T. DeGrand

(MILC Collaboration)

Physics Department, University of Colorado, Boulder, Colorado 80309

(Received 15 March 1999; published 17 September 1999)

A comparison is made of the (quenched) light hadron spectrum and of simple matrix elements for a hypercubic fermion action (based on a fixed point action) and the clover action, both using fat links, at a lattice spacing $a \approx 0.18$ fm. Renormalization constants for the naive and improved vector current and the naive axial vector current are computed using Ward identities. The renormalization factors are very close to unity, and the spectroscopy of light hadrons and the pseudoscalar and vector decay constants agree well with simulations at smaller lattice spacings (and with experiment). [S0556-2821(99)00519-6]

PACS number(s): 12.38.Gc, 11.15.Ha

I. INTRODUCTION

This paper is a continuation of earlier work [1,2] studying the properties of a particular type of improved action for studies of quenched QCD, with fermion-gauge-field couplings parametrized by ‘‘fat links,’’ and a lattice anomalous magnetic moment ‘‘clover’’ term. One of the actions studied here has fermionic couplings extending over a hypercube. The other action is the fat link clover action. Both actions are $O(a^2)$ improved. Features related to their chiral properties appear to be superior to those of standard discretizations, though this does not correspond to a realization of an exact lattice symmetry relation. The goal of this paper is to compare a particular implementation of a fixed point (FP) action for quenched QCD in four dimensions to a simpler improved action, via the usual tests of improvement. Much more elegant studies have been carried out in two dimensions [3]. The fat link clover action turns out to be an attractive alternative to the more complicated action.

The hypercubic action is inspired by the fixed point action program [4], applied to fermion actions for QCD in four dimensions [5–9]. FP actions are classically perfect, which means that they have the following desirable properties.

First, their spectrum has no lattice spacing a -dependent corrections of the form a^n for any n . Second, and probably more importantly, FP actions satisfy the Ginsparg-Wilson [10] remnant chiral symmetry condition, namely that the anticommutator of the propagator with γ_5 is a local operator. As a result, they suffer no additive quark mass renormalization and no multiplicative renormalization of axial vector currents [11], and satisfy the index theorem [12,13]. It would clearly be a desirable thing to have a version of such an action which could be used in numerical simulations, and this paper describes a candidate action which seems to satisfy all of the properties of a FP action very well, though not exactly.

The particular hypercubic action I will test is one whose free-field limit is constructed by blocking out of the continuum. It has the usual clover term, normalized to its tree-level value as described in [1]. The gauge connections of

both the hypercubic action and clover action I study are replaced by APE-blocked [14] links,

$$\begin{aligned}
 V_\mu^{(n)}(x) = & (1 - \alpha)V_\mu^{(n-1)}(x) + \alpha/6 \sum_{\nu \neq \mu} [V_\nu^{(n-1)}(x) \\
 & \times V_\mu^{(n-1)}(x + \hat{\nu})V_\nu^{(n-1)}(x + \hat{\mu})^\dagger + V_\nu^{(n-1)}(x - \hat{\nu})^\dagger \\
 & \times V_\mu^{(n-1)}(x - \hat{\nu})V_\nu^{(n-1)}(x - \hat{\nu} + \hat{\mu})], \quad (1)
 \end{aligned}$$

with $V_\mu^{(n)}(x)$ projected back onto $SU(3)$ after each step, and $V_\mu^{(0)}(n) = U_\mu(n)$ the original link variable. I take $\alpha = 0.45$ and $N = 10$ smearing steps, chosen because this fattening produces a very small additive mass renormalization.

There are two differences between this work and Ref. [1]. The first involves physics: since the completion of that work, we [2] have discovered that the properties of lattice QCD (specifically the spectrum of real fermion eigenmodes) changes as the lattice spacing coarsens, and that above about $a_{\max} \approx 0.2$ fm the would-be zero modes cannot be separated from the doubler modes. Since there is a qualitative change in the underlying dynamics, it does not seem to be appropriate to attempt to extrapolate to the continuum physics which involves chiral symmetry from lattice spacings greater than a_{\max} . The second difference is that in this paper I study FP operators, the analogues of the familiar ‘‘rotated’’ operators of the Symanzik program. For the action used in [1], the recursion relation for the FP operators is contaminated by a redundant eigenvector. I chose to find a different renormalization group transformation (blocking out of the continuum with a Gaussian blocking function) and a different hypercube action, the ‘‘Gaussian’’ hypercubic action, in order to construct the operators.

The outline of the paper is as follows: After reviewing the properties of FP actions, I discuss the ways that approximations to FP actions are imperfect. I summarize the physics features of fat link actions. Then I present tests of spectroscopy and of vector and axial vector current matrix elements, at lattice spacing $a = 0.18$ fm. I end with some conclusions and speculations.

II. QUICK REVIEW OF THE FIXED-POINT ACTION FORMALISM

To find a FP action for QCD, one begins with a set of fermionic $(\psi_n, \bar{\psi}_n)$ and gauge field $[U_\mu(n)]$ variables defined either on a fine lattice or in the continuum. The fine action is defined as

$$S = \beta S_g(U) + \bar{\psi}_i \Delta(U)_{ij} \psi_j. \quad (2)$$

S_g is the gauge action, i, j label sites, and $\Delta(U)$ is the fermion action. Introducing a renormalization group (RG) blocking kernel with a pure gauge piece T_g and a fermionic piece parametrized by a constant K and a blocking function $\alpha_{n_b, n}$ normalized by b ,

$$T = \beta T_g(U, V) + K \sum_{n_b} [\bar{\Psi}_{n_b} - \bar{\psi}_n (b \alpha_{n, n_b}^\dagger)] \times [\Psi_{n_b} - (b \alpha_{n_b, n'}) \psi_{n'}], \quad (3)$$

one integrates out the fine degrees of freedom to construct an action involving coarse-grained variables Ψ_{n_b} , $\bar{\Psi}_{n_b}$ and $V_\mu(n_b)$.

The renormalization group equation

$$e^{-S'} = \int d\psi d\bar{\psi} dU e^{-(T+S)} \quad (4)$$

has a pure gauge FP at $g^2=0$ ($\beta \rightarrow \infty$). In that limit the gauge action dominates the integral; its RG equation is given by the same steepest-descent equation as for a pure gauge model,

$$S^{FP}(V) = \min_{\{U\}} [S^{FP}(U) + T(U, V)], \quad (5)$$

while the fermions sit in the gauge-field background. The fermion action remains quadratic in the field variables, and the transformation of the fermion action is given most easily in terms of the propagator

$$[\Delta'(V)]_{n_b, n_b'}^{-1} = \frac{1}{K} \delta_{n_b, n_b'} + b^2 \alpha(U)_{n_b, n} [\Delta(U)]_{n, n'}^{-1} \alpha(U)_{n', n_b'}^T \quad (6)$$

where $\{U\}$ is the field configuration which minimizes Eq. (5) for a given $\{V\}$. For a blocking factor F , it is useful to rescale $b \alpha_{n_b, n} = F^{3/2} \Omega_{n_b, n}$ with the Fourier transform of $\Omega_{n_b, n}$ for a free theory normalized to $\Omega(q) \approx 1 + O(q^2)$. Then (again in free field theory) the momentum-space FP equation for the propagator becomes

$$[\Delta'(q)]^{-1} = \frac{1}{K} + \frac{1}{F} \sum_l \left| \Omega\left(\frac{q+2\pi l}{F}\right) \right|^2 \Delta\left(\frac{q+2\pi l}{F}\right)^{-1}. \quad (7)$$

Another useful quantity is the minimizing field, the value of the fine field (as a function of the coarse field) which minimizes the exponential in the Gaussian fermion integral:

$$\begin{aligned} \psi_{\min}(n) &= \zeta(n - F n_b) \Psi(n_b) \\ &= \sum_{m, m_b} \Delta^{-1}(n - m) b \alpha_{m, F m_b} \Delta(m_b - n_b) \Psi(n_b). \end{aligned} \quad (8)$$

A related object is the fixed-point field [4,15], a local average of fields which blocks into itself under a RG transformation (RGT),

$$\psi_{FP}(n) = \sum_m w(n - m) \psi(m). \quad (9)$$

The averaging function obeys the recursion relation

$$\sum_m w(F n_b - m) \zeta(m - F m_b) = \lambda w(n_b - m_b) \quad (10)$$

with $\lambda = 1/F^{3/2}$ carrying the canonical dimension of a fermion field. As the scale of the blocking transformation F goes to infinity, the FP field and minimizing field coincide. Correlators involving the FP field have no power-law cutoff effects—they are also classically perfect. Thus they play the same role for a FP action as the familiar ‘rotated operator’ does in the Symanzik improvement program.

The easiest way to find the FP field, for an action defined by an RG transformation with a scale factor F , is to solve Eq. (10) self-consistently for $w(n)$. Unfortunately, for the action studied in Ref. [1], with a blocking factor $F=2$ RGT, $\lambda = 1/F^{3/2}$ is not the leading eigenvalue: The leading eigenvector is $w(n) = \Delta(n)$, with an eigenvalue of about $2.56/2^{3/2}$. The phenomenon has been described by Kunszt in [16]. In terms of physics this does nothing: $w(n) = \Delta(n)$ just contributes a contact term to correlation functions. However, from an engineering point of view it is a serious problem, because it is quite difficult to determine the FP field by solving the recursive equation for w , and pulling out a nonleading eigenvector.

For a free field action constructed by blocking out of the continuum ($F \rightarrow \infty$ or, equivalently, m a continuous variable in the background of fixed n_b), the free FP field is readily constructed using the momentum-space version of Eq. (8). Therefore, because I wanted to study FP operators, I decided to construct a new action by following the MIT group [8,9] and blocking directly out of the continuum. There is a price associated with this—I can no longer solve FP equations for the propagator in a nontrivial gauge field background, as I did in [1]. I will follow a hybrid approach, of constructing the free field FP action, making it gauge invariant by using connections made of fat links, and just tuning the fattening to optimize the chiral properties of the action. The construction of the free action is described in the Appendix.

III. IMPERFECTION

A. Comparison to the standard tests of imperfection

A FP action is classically perfect, but an approximation to a FP action is not. It is thus an interesting exercise to ask how imperfect an approximate FP action will be.

One can approximately reconstruct the free field FP action and field by blocking out of the continuum. In Eq. (7) the $l=0$ term in the mode sum is the most singular for small q and the next higher order term is the $1/K$ term. Keeping only those contributions, a few lines of algebra yields

$$\Delta(q) = \frac{1}{\Omega(q)^2} \frac{-i\gamma \cdot q + m + \frac{q^2 + m^2}{K\Omega^2}}{1 + \frac{2m}{K\Omega^2} + \frac{q^2 + m^2}{(K\Omega^2)^2}} \quad (11)$$

$$\zeta(q) = \frac{1}{\Omega(q)^2} \frac{1 + \frac{i\gamma \cdot q + m}{K\Omega^2}}{1 + \frac{2m}{K\Omega^2} + \frac{q^2 + m^2}{(K\Omega^2)^2}}. \quad (12)$$

As $\Omega \sim 1 + q^2 + \dots$, the reader will recognize these formulas as rather baroque variations of the usual Symanzik-improved action and rotated field—up to an overall normalization constant. Indeed

$$\Delta \simeq \left(\gamma \cdot D + m - \frac{1}{K}(D^2 - m^2) \right) \left(1 - \frac{2m}{K} \right) + \dots \quad (13)$$

$$\zeta \simeq \left(1 + \frac{m - \gamma \cdot D}{K} \right) \left(1 - \frac{2m}{K} \right) + \dots \quad (14)$$

and so we identify the Wilson r parameter with $1/K = ra/2$.

The most serious lattice artifacts of a Wilson-like action come from its vertices. In the absence of an explicit construction of a FP action in a nontrivial background gauge field configuration, what can one say? First of all, a simple expansion of the action in powers of a shows that any hypercubic action made of thin or fat links has $O(a)$ contributions to its vertex, just like the Wilson action. These contributions must cancel in perturbation theory between the scalar vertices and an additional anomalous magnetic moment ‘‘clover’’ term, which of course is absent in the free theory.

In principle, the clover term could have any coefficient, but one fact we know is that the spectrum of a FP action is classically perfect. One can consider the spectrum of a fermion with infinitesimal momentum p in an infinitesimal external magnetic field B , $E = m_0 + p^2/2m_K - B/m_B + \dots$ and constrain $m_B = m_K = m_0$, by hand, if necessary. This constraint turns out to be identical to the requirement that the clover term have its usual tree level value. Now the calculation just paraphrases the old perturbative result of Heatlie *et al.* [17] and the result is as expected: the spectrum of a hypercubic approximation to a FP action, with the clover term, is improved through $O(a^2)$, and if matrix elements are measured using FP operators, they also have no $O(a)$ discretization errors.

B. Chiral properties

Violations of chiral symmetry in Wilson-like actions are an old story [18]: Write the fermion action as

$$\Delta(m) = \Delta_0 + m_0 \quad (15)$$

and consider a flavor nonsinglet chiral rotation $\psi(x) \rightarrow \exp[i\epsilon^a(x)(\lambda^a/2)\gamma_5]\psi(x)$, $\bar{\psi}(x) \rightarrow \bar{\psi}(x)\exp[i\epsilon^a(x)(\lambda^a/2)\gamma_5]$. The Ward identity for this rotation is

$$\begin{aligned} \frac{\delta \langle O(x_1, \dots, x_n) \rangle}{\delta \epsilon^a(x)} &= \langle O(x_1, \dots, x_n) \partial_\mu J_\mu^5(x)^a \rangle \\ &\quad - \left\langle O(x_1, \dots, x_n) m_0 \bar{\psi}(x) \frac{\lambda^a}{2} \gamma_5 \psi(x) \right\rangle \\ &\quad - \left\langle O(x_1, \dots, x_n) \left(\bar{\psi}(x) \frac{\lambda^a}{2} \{ \gamma_5, \Delta_0 \} \psi(x) \right) \right\rangle. \end{aligned} \quad (16)$$

The last term is the lattice artifact. In a generic non-FP action, it will mix with lower-dimensional operators

$$\begin{aligned} \bar{\psi}(x) \{ \gamma_5, \Delta_0 \} \psi(x) &= (1 - Z_A) \partial_\mu J_\mu^5(x) + \Delta m \psi(x) \gamma_5 \psi(x) \\ &\quad + O(a) + \dots \end{aligned} \quad (17)$$

to give a nonzero additive renormalization to the quark mass and an overall multiplicative renormalization to the axial current. It is also responsible for the mixing of opposite parity operators in matrix elements appropriate to, for example, B_K . In perturbation theory all of these mixings are due to one-loop graphs and are $O(g^2)$.

The Ginsparg-Wilson relation eliminates these mixings and renormalizations [12] (or to be more precise converts them into local corrections to the Ward identities), by canceling the propagator connecting the operator to the current with the anticommutator against the action term from the anticommutator.

The ingredient of an approximate FP action most necessary to reproduce this feature of a FP action is a fat link. The dominant graphs contributing to $Z_A - 1$ and Δm contain tadpoles, whose contributions from large q^2 are suppressed by the soft $q\bar{q}g$ vertices of a fat link action [2]. The presence of the fat link in the one explicit realization of the Ginsparg-Wilson relation, the ‘‘overlap action’’ [19]

$$\Delta = \frac{K}{2} \left[1 - \left(1 - \frac{2}{K} \Delta_0 \right) / \sqrt{\left| 1 - \frac{2}{K} \Delta_0 \right|^2} \right], \quad (18)$$

using a thin link Δ_0 , can be seen easily by making a hopping parameter expansion in Δ_0 .

Finally, can one quantify the size of chiral violations expected for an approximate FP action? Imagine constructing a FP action by beginning with the Wilson action and performing a series of factor-of-2 RGT’s. The Wilson term violates the Ginsparg-Wilson relation. It is a dimension-5 operator, and so under each blocking step its size decreases by a factor of 1/2. After N blocking steps the action will have a range $O(N)$ and the size of the violating operator will be $O(\exp(-N \ln 2))$. This exponential decrease of chiral viola-

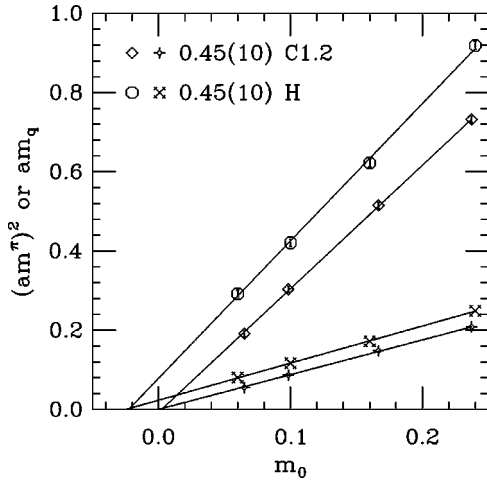


FIG. 1. m_π^2 and the quark mass vs bare quark mass for various fermion actions. Data are diamonds and small plusses with circles at their centers for m_π^2 and the quark mass from the PCAC (partial conservation of axial vector current) relation respectively, for the fat link clover action of Ref. [2], with the clover term boosted by a factor of 1.2, and octagons and fancy crosses for the Gaussian hypercubic action. Both actions have fat links with $\alpha=0.45$, $N=10$. The lines represent naive linear fits of $(am_\pi)^2$ or am_q vs the bare quark mass am_0 .

tions with range of the action seems superficially to be the same behavior as is seen with domain wall fermions (where N is the length of the fifth dimension [20]). One can easily see this behavior in explicit calculations using free field theory.

IV. TUNING FOR CHIRAL BEHAVIOR

The most visible aspect of bad chiral behavior for Wilson-like fermions is the presence of exceptional configurations, which arise when the Dirac operator Δ_0 has a real eigenmode at $\lambda = -m$, a value which happens to coincide with the bare mass m at which one attempts to construct a propagator for $\Delta_0 + m$ [21]. We have argued in Ref. [2] that an action whose gauge connections are fat links has a narrower range of real eigenvalues than a thin link action does.

In Ref. [2] we proposed a method for tuning an action to optimize its chiral behavior. This involved measuring the spread of real eigenmodes of the Dirac operator, and varying the amount of fattening and the size of the clover term to narrow the spread of real eigenmodes. This is computationally costly and, if the amount of fattening is large, produces

TABLE I. Best-fit masses, Gaussian hypercube action, $\beta = 3.70$ ($aT_c = 1/4$).

am_q	PS	V	N	Δ
0.32	1.116(3)	1.246(5)	1.935(11)	2.040(12)
0.24	0.959(5)	1.117(6)	1.726(10)	1.862(16)
0.16	0.789(6)	0.994(8)	1.517(13)	1.735(17)
0.10	0.649(6)	0.902(13)	1.370(15)	1.622(23)
0.06	0.541(7)	0.851(19)	1.264(21)	1.543(29)

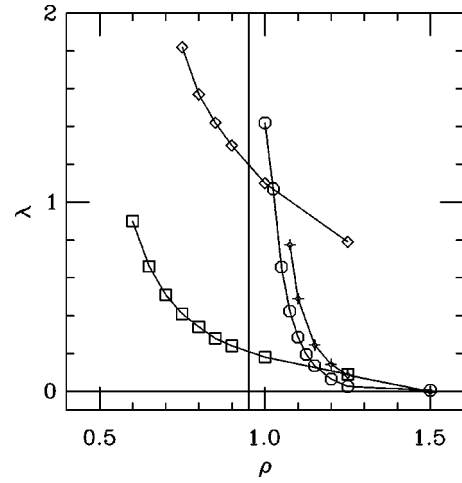


FIG. 2. Smallest real eigenmode of the massless Dirac operator vs instanton size for various fermion actions. Diamonds and squares show the usual thin-link Wilson and clover actions while the small plusses with circles at their centers show the fat link clover action and octagons show the hypercubic action (both with fattening $\alpha = 0.45$ and $N=10$ steps).

only the unsurprising result that a clover coefficient close to the tree-level value is the optimum one.

Here, I take a simpler (though more tasteless) approach: fix the clover coefficient to its tree-level value and vary the amount of fattening until the additive mass renormalization, measured naively by extrapolating the squared pion mass linearly to zero, appears to be small. This is done at small quark masses, but not at masses which are so small that the quenched approximation breaks down due to the presence of unpaired instanton modes [22]. The results are shown in Fig. 1. Data are diamonds and small plusses with circles at their centers for m_π^2 and the quark mass from the PCAC (partial conservation of axial vector current) relation respectively, for the fat link clover action of Ref. [2], with the clover term boosted by a factor of 1.2, and octagons and fancy crosses for the Gaussian hypercubic action. Both actions have fat links with $\alpha=0.45$, $N=10$. A jackknife fit of the four lightest masses of $m_\pi^2 = A(m_0 - m_c)$ or $m_q = A(m_0 - m_c)$ (this is the lattice quark mass from the PCAC relation; see Sec. VI C) gives $m_c = -0.0226(15)$ from m_π^2 and $m_c = -0.0248(7)$ from the quark mass, for the hypercubic action, and $m_c = 0.0023(19)$ and $-0.0002(18)$ for the fat link clover action.

TABLE II. Best-fit masses, fat link clover action, $\beta = 3.70$ ($aT_c = 1/4$).

κ	PS	V	N	Δ
0.114	1.094(3)	1.226(4)	1.887(10)	1.984(9)
0.116	0.977(3)	1.137(5)	1.741(9)	1.862(12)
0.118	0.856(5)	1.048(6)	1.595(10)	1.740(16)
0.120	0.718(5)	0.960(9)	1.449(12)	1.616(25)
0.122	0.551(7)	0.866(18)	1.280(19)	1.555(25)
0.123	0.437(7)	0.807(28)	1.190(30)	1.482(32)

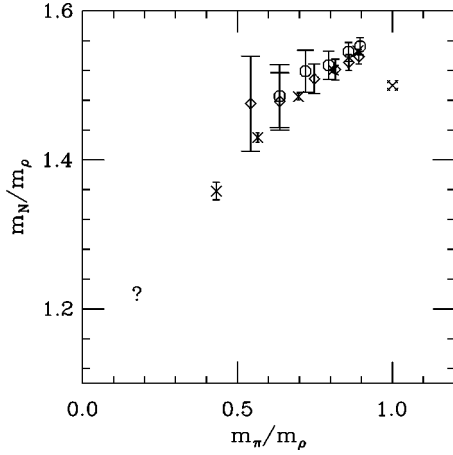


FIG. 3. Edinburgh plot showing $\beta=6.15$ staggered fermions from Ref. [25] (crosses), the fat link clover action (diamonds) and the Gaussian hypercube action (octagons).

To make a controlled comparison of the zero mode spectra of these actions, I show in Fig. 2 the real eigenmode spectrum of several of these actions on a family of single instanton configurations. The construction of the instantons is described in Ref. [23]. They are $SU(2)$ instantons in singular gauge centered at $(L/2+1/2, L/2+1/2, L/2+1/2, L/2+1/2)$ in a periodic lattice of size $L=8$. The vertical line at $\rho \approx 0.95$ marks the smallest radius visible to the approximate FP gauge action of Ref. [1]. Diamonds and squares show the usual thin-link Wilson and clover actions while the other plotting symbols show fat link actions. As the instantons

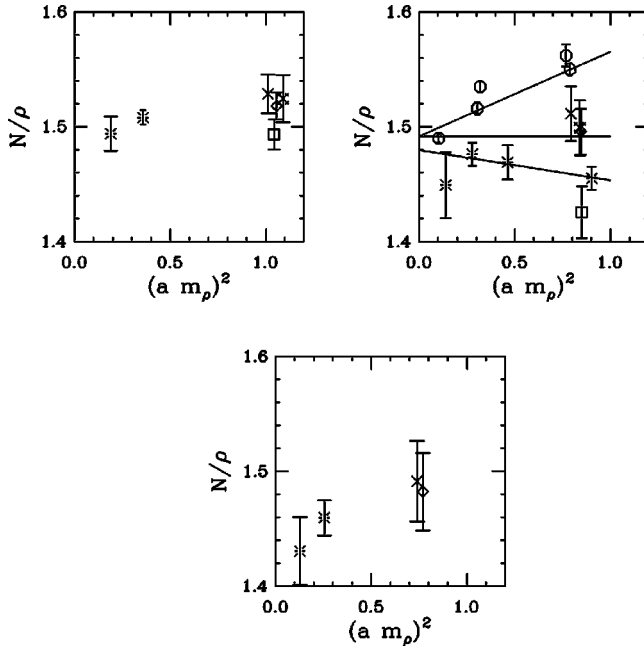


FIG. 4. N/ρ mass ratio interpolated to $\pi/\rho=0.80$ (a), 0.70 (b), 0.65 (c). Shown are the nonperturbatively improved (thin-link) clover action (bursts), $c_{sw}=1.2$ fat link clover action (squares on $\beta=5.7$ Wilson gauge actions, diamonds on FP gauge configurations), hypercubic action of Ref. [1] (fancy crosses), and Gaussian hypercubic action (crosses). Octagons are $\beta=6.15$ staggered simulations.

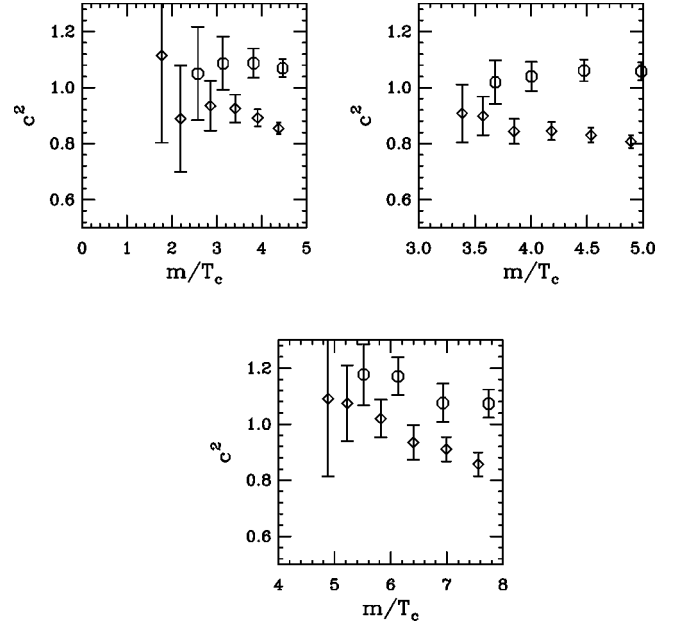


FIG. 5. c^2 for the fat link clover action (diamonds) and Gaussian hypercubic action (octagons), for (a) pseudoscalar (b) vector and (c) nucleon correlators. Hadron masses are shown in units of the deconfinement temperature $T_c=1/(4a)$.

shrink, the smallest real eigenmode becomes more positive, and then, when the instanton disappears, it collides with another real eigenmode (a doubler) to produce a complex conjugate pair of eigenvalues.

For future reference, recall that an action obeying the Ginsparg-Wilson relation would have a zero eigenmode on a topologically nontrivial configuration, but when the instanton “falls through the lattice” the eigenmode should jump discontinuously to some positive value. Presumably the more improved an action is, the sharper the rise of the real eigenmode as the instanton size shrinks. All fat link actions, both hypercube and clover, satisfy that criterion. Based on our studies with fat link clover actions [2], we believe that this feature, like the small mass renormalization, is caused by the fat link, not by features of the fermion action which could be seen in the free-field limit.

V. NUMERICAL TESTS

A. Spectroscopy

I carried out quenched spectroscopy on a set of $80 \times 8^3 \times 24$ background gauge field configurations with a lattice spacing $a \approx 0.18$ fm using the approximate FP gauge action of Ref. [1], at $\beta=3.70$. As a fiducial test of a simpler action I recomputed the spectrum of the fat link clover action of Ref. [2] on the same set of background configurations (in order to remove all effects of the gauge fields from comparisons). This action also has $\alpha=0.45$, $N=10$ APE-smearred fat links and its clover term is rescaled by a factor $C_{SW}=1.2$.

The cost of the hypercubic action compared to the clover action is a factor of about 17 per multiplication $\psi=(\Delta+m)\chi$ during the iterative construction of the propagators. Both the fat link clover action and hypercubic actions appear

TABLE III. $R_{\pi,0}^{X,Y}$, Gaussian hypercube action, $\beta=3.70$ ($aT_c=1/4$).

am_q	$R_{\pi,0}^{C,L}(\vec{q}=0)$	$R_{\pi,0}^{C,L}(\vec{q}=2\pi/8)$	$R_{\pi,0}^{C,I}(\vec{q}=0)$	$R_{\pi,0}^{C,I}(\vec{q}=2\pi/8)$	$R_{\pi,0}^{I,L}(\vec{q}=0)$	$R_{\pi,0}^{I,L}(\vec{q}=2\pi/8)$
0.32	0.970(1)	1.01(2)	1.074(1)	1.19(1)	0.906(2)	0.87(2)
0.24	0.971(1)	1.11(2)	1.081(1)	1.24(1)	0.899(2)	0.91(1)
0.16	0.971(1)	1.03(3)	1.088(1)	1.24(1)	0.892(3)	0.86(1)
0.10	0.971(1)	1.42(8)	1.094(1)	1.35(2)	0.868(3)	0.99(3)

to require about half the number of iterations as the usual thin link clover action to converge to the same residue $|\psi - (\Delta + m)\chi|^2/|\chi|^2$, presumably because their high Fourier modes decouple from the gauge fields. Neither of these actions developed any exceptional configurations over the studied range ($\pi/\rho \geq 0.54$ and 0.64). In Ref. [2] we did a scan of $80 \cdot 8^3 \times 24$ $\beta=5.7$ Wilson gauge action configurations with the fat link clover action and the thin link clover action with nonperturbative $C_{sw}=2.25$ and found no exceptional configurations for the fat link action for $m_\pi/m_\rho \geq 0.4$ ($am_\pi \geq 0.3$) while 11 configurations were exceptional for the thin link action.

The spectrum analysis is completely standard [1]. Both actions reproduce the results of spectroscopy calculations of more conventional actions at smaller lattice spacings. The spectroscopy is tabulated in Tables I and II.

To show the data graphically, I begin with an Edinburgh plot, Fig. 3, containing $\beta=6.15$ staggered fermion data [24] and data from the two actions shown here, the fat link clover action and the Gaussian hypercubic action. I compare scaling violations in hyperfine splittings by interpolating the data to fixed π/ρ mass ratios and plotting the N/ρ mass ratio vs $m_\rho a$. I do this at three π/ρ mass ratios, 0.80, 0.70, and 0.65, in Fig. 4. The bursts are from the nonperturbatively improved (thin link) clover action of Refs. [25] and [26]. The octagons show data from staggered fermions at $\beta=6.15$. The other plotting symbols show our test actions: They are the hypercubic action of Ref. [1] (fancy crosses) and of this work (crosses) and the $c_{sw}=1.2$ fat link clover action (squares on $\beta=5.7$ Wilson gauge actions [2], diamonds on FP gauge configurations). The data indicate that the improved kinetic properties of the hypercubic action do not affect hyperfine splittings very strongly. The two outer straight lines in the figure are linear fits in $(am_\rho)^2$ to the staggered and nonperturbatively improved clover data. The inner straight line is a constant at the value of the extrapolated $a=0$ value of the staggered data.

The fat link clover action on Wilson gauge configurations has a slightly larger hyperfine splitting than the other actions. Could this be an effect of the gauge action on the spectrum? Could it be due to the fact that the Wilson gauge action overproduces small instantons compared to the FP gauge action?

Differences appear when one compares the dispersion relations (Fig. 5). The squared speed of light, $c^2 = [E(p)^2 - m^2]/p^2$, for $\vec{p} = 2\pi/8(1,0,0)$, is computed by performing a correlated fit to the two propagators, one at the nonzero \vec{p} , the other at $\vec{p}=0$. At larger mass the clover action's c^2 falls away from unity while the hypercubic action shows a fairly

constant $c^2 - 1 \approx 0.025$. To achieve the same mismatch of $c^2 - 1$ as the hypercubic action, at the same m/T_c , one would have to decrease the lattice spacing by about a factor of roughly 2 [assuming $c^2 - 1 \approx O(a^2)$].

B. Vector currents

There are many definitions of conserved currents. The simplest one is constructed by writing [10,12] $U_\mu(n) = 1 + igA_\mu(n) + \dots$ and defining

$$J_\mu(n) = -i \frac{\delta S}{\delta A_\mu(n)}. \quad (19)$$

In these actions I have replaced the thin links by fat links, $V_\mu(n) = 1 + igB_\mu(n) + \dots$, which in linear approximation corresponds to

$$B_\mu(n) = \sum_{r,\nu} c_{\mu\nu}(r) A_\nu(r) \quad (20)$$

for some smearing function $c_{\mu\nu}(r)$. It is more convenient to replace Eq. (19) with a ‘‘fat conserved current’’

$$\hat{J}_\mu(n) = -i \frac{\delta S}{\delta B_\mu(n)}. \quad (21)$$

Are $\partial_\mu J_\mu(n) = 0$ and $\partial_\mu \hat{J}_\mu(n) = 0$ consistent? Yes. In general, $c_{\mu\nu}$ has two parts. The first is a term proportional to $\delta_{\mu\nu}$, which is parity even [$\delta_{\mu\nu} c_S(r) A_\mu(r)$ with $c_S(r+\hat{\lambda}) = c_S(r-\hat{\lambda})$], and a term which is proportional to $(1 - \delta_{\mu\nu}) c_A(r) A_\nu(r)$ with $c_A(r+\hat{\lambda}) = -c_A(r-\hat{\lambda})$. The ‘‘1’’ terms in $1 - \delta_{\mu\nu}$ are of the form $\sum_{r,\nu} c_A(r) [J_\nu(n+r) - J_\nu(n+r-\nu)]$ which vanishes if J_μ is conserved, and so $\hat{J}_\mu(n) = \sum_r d(r) J_\mu(n+r)$ for some function $d(r)$. Thus conservation of the usual current implies (all rather trivially) conservation of the associated fat current.

In what follows, the conserved vector current is defined using Eq. (21). The hypercubic action has a ‘‘conventional’’

TABLE IV. $R_\rho^{X,Y}$, Gaussian hypercube action, $\beta=3.70$ ($aT_c=1/4$).

κ	$R_\rho^{C,I}(\vec{q}=0)$	$R_\rho^{I,L}(\vec{q}=0)$	$R_\rho^{I,L}(\vec{q}=2\pi/8)$
0.116	0.574(9)	0.933(1)	0.938(2)
0.118	0.621(13)	0.930(1)	0.931(2)
0.120	0.669(4)	0.925(1)	0.925(3)
0.122	0.732(7)	0.920(1)	0.921(4)

TABLE V. $R_{\pi,0}^{X,Y}$, fat link clover action, $\beta=3.70$ ($aT_c=1/4$).

κ	$R_{\pi,0}^{C,L}(\vec{q}=0)$	$R_{\pi,0}^{C,L}(\vec{q}=2\pi/8)$	$R_{\pi,0}^{C,I}(\vec{q}=0)$	$R_{\pi,0}^{C,I}(\vec{q}=2\pi/8)$	$R_{\pi,0}^{L,L}(\vec{q}=0)$	$R_{\pi,0}^{L,L}(\vec{q}=2\pi/8)$
0.116	1.308(17)	1.349(4)	1.136(2)	1.026(4)	1.2383(1)	1.301(1)
0.118	1.227(3)	1.449(3)	1.009(2)	1.254(4)	1.216(1)	1.26(1)
0.120	1.116(3)	1.262(12)	1.003(3)	1.43(5)	1.149(2)	1.15(1)
0.122	1.080(6)		0.995(5)		1.084(1)	

normalization $S = m\bar{\psi}\psi + \dots$, in contrast to the ‘‘kappa’’ normalization of the clover action $S = \bar{\psi}\psi - \kappa\bar{\psi}D\psi$. In either case, the local current is $\bar{\psi}\gamma_\mu\psi$ and the improved current is $(\bar{\zeta}\psi)\gamma_\mu(\zeta\psi)$.

Now recall the classification of definitions of the current [27]:

$$\langle f|J_\mu|i\rangle_{cont} = Z_{J^X}\langle f|J_\mu^X|i\rangle_{latt} + O(a) + O(g^2a) + \dots \quad (22)$$

where $Z_{J^X} = F(m)(1 + c_1g^2 + \dots)$ (introducing the field rescaling of the usual Wilson or clover actions). If the current is conserved (C), its $Z=1$. If it is improved (I), the $O(a)$ term is zero. The conserved current of either action is not improved. The ‘‘rotated’’ or FP currents are improved but not conserved. It is conventional to rescale the results of the clover action so that $F(m=0)=1$. This amounts to rescaling the clover field $\psi \rightarrow \sqrt{2}\kappa\psi$. I will present all results that way even though it is unnecessary for this method of finding renormalization factors.

I measured three kinds of matrix elements:

$$R_\pi^X = \frac{\langle \pi(T)|\pi(0)\rangle}{\langle \pi(T)|J_0(t)^X|\pi(0)\rangle}, \quad (23)$$

$$R_{\pi,\vec{q}}^{X,Y} = \frac{\langle \pi(T,0)|J_0(t,\vec{q})^X|\pi(0,-\vec{q})\rangle}{\langle \pi(T,0)|J_0(t,\vec{q})^Y|\pi(0,\vec{q})\rangle}, \quad (24)$$

and the ratio

$$R_\rho^{X,Y}(\vec{q}) = \frac{\langle 0|J_i^X|V(\vec{q})\rangle}{\langle 0|J_i^Y|V(\vec{q})\rangle}. \quad (25)$$

Note that $\langle 0|J_i|V\rangle = \hat{\epsilon}_i m_V^2/f_V$ gives the vector meson decay constant f_V . Naively speaking, $R_\pi^X = Z_{V^X}$ and $R_\pi^{X,Y} = Z_{V^Y}/Z_{V^X}$.

Equation (24) is measured for $0 < t < T$ with $T=10$ on $8^3 \times 24$ lattices (20 for the hypercube and 40 for the clover action), on a subset of the bare quark mass values, and Eq. (25) is a by-product of spectroscopy. The source at $t=0$ is a Gaussian shell source centered on the origin; the sink at T is a point sink projected onto zero momentum, and momentum was injected at the current. I was able to get a signal for $\vec{q} = (2\pi/8)(1,0,0)$ in addition to $\vec{q}=0$. Fits of $R_{\pi,\vec{q}}^{X,Y}$ are done by a correlated fit to the two three-point functions, fits of

$R_{\pi,\vec{q}}^{X,Y}$ are done by single-elimination jackknife and fits of $R_\rho^{X,Y}$ by a correlated fit to the two two-point functions.

The renormalization factors are determined sequentially. I begin with a forward matrix element R_π^X of the conserved current: current conservation demands that this ratio be equal to unity, or $Z_{J^C}=1$. Confirming that measurement, I can use Eq. (23) or (24) (at $\vec{q}=0$) to determine Z_V 's for the other currents. Self-consistency for lattice perturbation theory demands that the Z 's should be process independent, but in general that will not be true: the $O(a)$ corrections to Eq. (22) will make the ratios process dependent. The absence of process dependence in the ratios of Z 's is a measure of improvement.

By itself, the ratio R_π^X is contaminated by wraparound in time. The wraparound mostly affects the two point function and it can be corrected for, by fitting the two-point function to a hyperbolic cosine ($\approx A\{\exp(-\mu t) + \exp[-\mu(N_t - t)]\}$) and the three-point function to a forward-going exponential $\approx A/Z \exp(-\mu T)$.

Tables III and IV show the results for measurements of Eqs. (25) and (24) for the hypercube action, and the same results for the fat link clover action are in Tables V and VI. Figures 6 and 7 illustrate the results. All the fat link Z factors are close to unity. In contrast, $Z_V^I \approx 0.78$ for the nonperturbatively improved thin link clover action at $\beta=6.0-6.2$ [28].

Tables III and V show that the ratio of the conserved current to either the local or improved currents is quite different at $\vec{q}=0$ and $\vec{q}\neq 0$. This is an artifact of the imperfection of the conserved current. Although the ratio of the local current to the improved current is also $O(a)$, its momentum dependence is much smaller. The conserved current also does not respond well to being folded over into $\langle 0|J_i|\rho\rangle$. In Tables IV and VI, I show only the $\vec{q}=0$ ratio with the improved current: it is quite different from the ratio of forward matrix elements.

Figure 7 shows a comparison of different measurements of Z_{V^L}/Z_{V^I} from two point and three point functions. The scatter of the points for the hypercubic action is small and

TABLE VI. $R_{\rho,0}^{X,Y}$, fat link clover action, $\beta=3.70$ ($aT_c=1/4$).

κ	$R_\rho^{C,I}(\vec{q}=0)$	$R_\rho^{L,L}(\vec{q}=0)$	$R_\rho^{L,L}(\vec{q}=2\pi/8)$
0.116	0.732(22)	0.978(1)	0.973(1)
0.118	0.725(35)	0.986(1)	0.982(1)
0.120	0.714(18)	0.993(1)	0.989(1)
0.122	0.722(26)	0.997(1)	0.994(1)

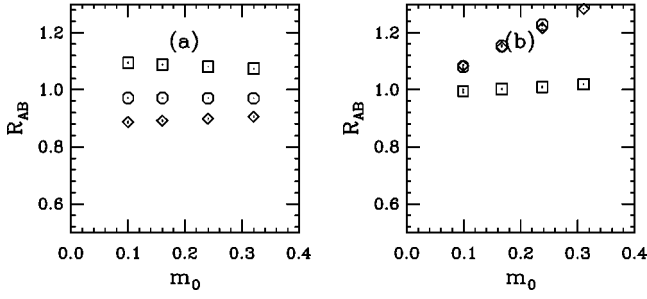


FIG. 6. Ratios of three-point functions at $\vec{p}=0$ from (a) the hypercubic action and (b) the fat link clover action. Octagons label $R^{C,L}$, squares $R^{C,I}$, and diamonds $R^{I,L}$.

appears to be mass independent. In contrast, the Z factors of the fat link clover action two-point and three-point functions are quite different, especially at higher mass, although they appear to extrapolate into each other at zero quark mass. One could argue that since the local current has $O(a)$ errors, and the improved current is $O(a^2)$, we are just seeing an $O(a)$ effect and the improved current is the one to use. However, the same argument should apply to the hypercubic action, and there the effects are much smaller. If it is an $O(a)$ effect, one will need more than a factor of 2 reduction in the lattice spacing (or in $m_0 a$) to make the fat link clover action as consistent as the hypercubic action.

Finally, I can compare $1/f_V$ to the observed vector meson decay widths, by multiplying the lattice value (given in Table VII or VIII) by the appropriate Z factor (extracted from the $\vec{q}=0$ $R_{\pi,0}^{C,X}$ correlator—the first or third column of Table III or V). The result is shown in Fig. 8(a). All the currents bracket the ϕ meson decay constant quite nicely, although there is considerable uncertainty in the fat link clover result due to the different renormalization factors. Vector decay constants have also been computed using the thin link clover action, with a nonperturbatively tuned clover term, at smaller lattice spacings (Wilson gauge action, $\beta=6.0$ and 6.2), in Ref. [25]. I plot a comparison between those values and the results of this simulation (showing only the improved operator, to avoid clutter) in Fig. 8(b). There does not seem to be much to be gained for this matrix element by going to the smaller lattice spacings.

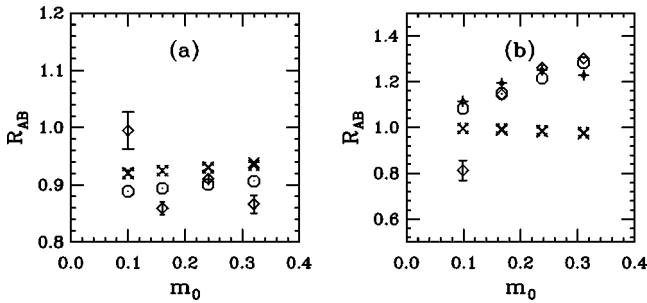


FIG. 7. $R^{I,L}$ from ratios of three point functions [octagons $\vec{q}=0$, diamonds $\vec{q}=(2\pi/8,0,0)$, small pluses with circles at their centers, $\vec{q}=(2\pi/8,2\pi/8,0)$] and two-point functions [fancy crosses $\vec{q}=0$, crosses $\vec{q}=(2\pi/8,0,0)$]. (a) Hypercubic action, (b) fat link clover action.

TABLE VII. Lattice $1/f_V$ for the hypercubic action.

Mass	Local	Improved
0.32	0.188(2)	0.177(2)
0.24	0.203(3)	0.191(3)
0.16	0.226(3)	0.210(3)
0.10	0.239(4)	0.222(3)

C. Axial vector current

I have performed a nonperturbative determination of the axial vector current renormalization factor following the classical approach of Martinelli and Maiani [29]. This begins with the Ward identity, Eq. (16), with the operator $O = A_v^b(y)V_\rho^c(z)$ where $V_\rho^c(z) = \bar{\psi}(z)(\lambda^c/2)\gamma_\rho\psi(z)$ and $A_v^b(y) = \bar{\psi}(z)(\lambda^b/2)\gamma_\nu\gamma_5\psi(y)$. Standard manipulations lead to the identity

$$\begin{aligned}
2m_q \sum_n \sum_y \langle P^a(n) A_v^b(\vec{y}, y_0) V_\rho^c(0,0) \rangle \\
= -if^{abd} \sum_y \langle V_v^d(\vec{y}, y_0) V_\rho^c(0,0) \rangle \\
- if^{acd} \sum_y \langle A_v^b(\vec{y}, y_0) A_\rho^d(0,0) \rangle. \quad (26)
\end{aligned}$$

[$P^a(n)$ is the pseudoscalar current $\bar{\psi}(n)(\lambda^a/2)\gamma_5\psi(n)$.] To pass to a lattice description, all currents are rescaled $J \rightarrow Z_L J_L$ and the quark mass is replaced by the unnormalized quark mass from the lattice PCAC relation, $m_q \rightarrow \rho = m_q Z_P / Z_A$ with

$$2\rho = \frac{\sum_y \langle \partial_0 A_0(\vec{y}, y_0) C(0,0) \rangle}{\sum_y \langle P(\vec{y}, y_0) C(0,0) \rangle} \quad (27)$$

computed through a (correlated) fit to two two-point functions. The lattice Ward identity then becomes

$$-2\rho \langle PAV \rangle = \frac{Z_V}{Z_A} \langle VV \rangle - \frac{1}{Z_V} \langle AA \rangle. \quad (28)$$

(I computed Z_A for the local axial vector current; the Ward identity for the improved current involves additional contact terms.) As for the vector current, I evaluated the two point

TABLE VIII. Lattice $1/f_V$ for the fat link clover action.

κ	Local	Improved
0.116	0.162(2)	0.159(2)
0.118	0.181(2)	0.179(2)
0.120	0.203(4)	0.201(3)
0.122	0.236(4)	0.235(4)

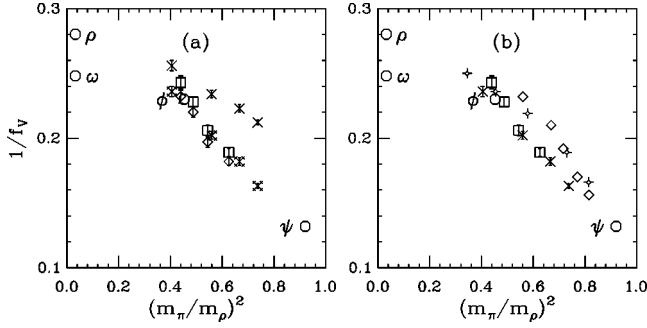


FIG. 8. (a) Vector meson decay constants at $a=0.18$ fm from the hypercubic and fat link clover actions. Diamonds and squares are the local and improved operator with the hypercubic action while the crosses and fancy crosses are the same operators with the fat link clover action. (b) A comparison of $1/f_V$ using improved operators with the hypercubic action (crosses), the fat link clover action (squares), and the nonperturbatively tuned thin link clover action at $\beta=6.0$ (diamonds) and 6.2 (small crosses with circles) from Ref. [26].

functions and the three point function with a source on $t=0$ and a sink on $t=y_0=10$. I used 40 hypercubic propagators and 80 fat link clover propagators, taking the local Z_V from the forward current matrix element (rightmost data column of Tables III and V). I only looked at three lighter quark masses. Correlated fits to the appropriate two point functions, Eqs. (27) and a correlated fit extracting $\langle 0|A_0|PS\rangle = f_{PS}m_{PS}$, produced the results shown in Tables IX and X. The two errors on Z_A are from the jackknife and from the variation of ρ and Z_V . I use $a\sqrt{\sigma}=0.4049(37)$ from Ref. [1] to connect the lattice spacing a and string tension σ . In the last column, I quote a physical number using a nominal $\sqrt{\sigma}=440$ MeV. A linear extrapolation to the chiral limit in the quark mass produces the bottom line. The agreement with experiment from the hypercube action for the pion seems acceptable. Notice that Z_A shows a mild mass dependence and that, in the chiral limit, it is also quite close to unity. The clover action shows a smaller mass dependence. In contrast, the nonperturbatively tuned thin link clover action Z_A from the rotated operator is 0.79 at Wilson gauge action $\beta=6.0$ [28].

VI. CONCLUSIONS

Few of the results shown here are surprising. The hypercube action is designed to show improved chiral and kinetic properties, and it does. The fat link clover action has poorer kinetic properties, but in the small mass limit they can be

TABLE IX. Lattice axial vector parameters for the hypercube action.

Mass	af_{PS}	Z_A^L	$f_{PS}/\sqrt{\sigma}$	f_{PS} (MeV)
0.24	0.170(2)	0.865(1)(1)	0.3632(55)	160(3)
0.16	0.156(2)	0.902(2)(2)	0.3475(60)	153(3)
0.10	0.147(2)	0.916(2)(2)	0.3326(55)	146(3)
0		0.966(3)		134(6)

TABLE X. Lattice axial vector parameters for the fat link clover action.

κ	af_{PS}	Z_A^L	$f_{PS}/\sqrt{\sigma}$	f_{PS} (MeV)
0.118	0.135(2)	0.851(33)(4)	0.283(13)	124(7)
0.120	0.134(2)	0.870(79)(4)	0.288(30)	127(13)
0.122	0.130(3)	0.872(28)(4)	0.280(12)	123(5)
0		0.89(5)		122(10)

compensated for by going to a smaller lattice spacing. Both actions have vector and axial vector current renormalization factors which are very close to unity.

It is an open question to me as to whether the hypercube action is a practical improvement over the simpler alternative of the fat link clover action. The cost of the action is a factor of 17 per computation of $\psi=\Delta\chi$ compared to the usual clover action, with a gain that typically only half as many steps of the inversion algorithm are required to construct Δ^{-1} . The fat link clover action [2] has all the gain with no additional cost. Of course, its kinetic properties are not improved, and so one must reduce the lattice spacing to improve the dispersion relation and scaling behavior of matrix elements. Heavy quark physics with the fat link clover action will suffer from the same kinetic artifacts as the standard clover action.

A potential use for the hypercube action is to construct an action which realizes the Ginsparg-Wilson (GW) action exactly. That is an active area of research [30], with most attempts involving an iteration using the Wilson action as a zeroth-order action. The eigenmodes of a GW action lie on or close to a circle. The thin link Wilson action and even the clover action seem to be poor choices for a zeroth-order action, because their free-field eigenvalue spectrum does not look anything like a circle, and because their real eigenmode spectrum in background instanton configurations does not look anything like a step function (recall Fig. 2). The fat link stiffens the real eigenmode spectrum on instantons. A hypercube action like the one described here looks like a much

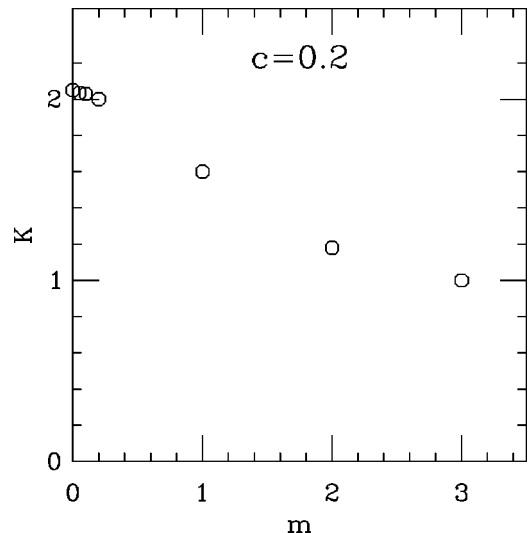


FIG. 9. Optimum K defining the RT of the massive action.

TABLE XI. Couplings of the hypercubic action used in this work. The free action is parametrized as $\Delta = \lambda(r) + i\gamma_\mu \rho_\mu(r)$.

$\lambda(r)$	
Offset	
1 0 0 0	$-0.0725 \exp(-0.7092m - 0.0149m^2)$
1 1 0 0	$-0.0319 \exp(-1.007m - 0.0421m^2)$
1 1 1 0	$-0.0156 \exp(-1.123m - 0.0803m^2)$
1 1 1 1	$-0.0080 \exp(-1.180m - 0.1169m^2)$
$\rho_0(r)$	
Offset	
1 0 0 0	$-0.1819 \exp(-0.9475m + 0.0031m^2)$
1 1 0 0	$-0.0318 \exp(-1.031m - 0.0502m^2)$
1 1 1 0	$-0.00897 \exp(-1.017m - 0.1047m^2)$
1 1 1 1	$-0.00295 \exp(-0.9307m - 0.1633m^2)$

better choice, provided of course the cost of its use is less than the gain in number of iteration steps.

Finally, dynamical fermion simulations with fat link actions still appear [31] to require smaller levels of fattening than are needed to substantially improve the chiral properties of Wilson-type actions. But for quenched calculations either action seems to me to be superior to a thin link action.

ACKNOWLEDGMENTS

I would like to thank Anna Hasenfratz, Tamas Kovacs, and the members of the MILC Collaboration for useful conversations and C. Sachrajda and J. Skullerud for instructive correspondence. This work was supported by the U.S. Department of Energy, with some computations done on the T3E at Pittsburgh Supercomputing Center through resources awarded to the MILC Collaboration, and on the Origin 2000 at the University of California, Santa Barbara.

TABLE XII. The hypercubic approximation to the FP field for the hypercubic action used in this work. The field is parametrized as $\zeta = \lambda(r) + i\gamma_\mu \rho_\mu(r)$.

$\lambda(r)$	
Offset	
0 0 0 0	$0.1047 + 0.3287m - 0.0639m^2$
1 0 0 0	$\exp(-3.4070 - 0.6776m - 0.0639m^2)$
1 1 0 0	$\exp(-4.2303 - 0.9708m - 0.07609m^2)$
1 1 1 0	$\exp(-4.9495 - 1.0860m - 0.1147m^2)$
1 1 1 1	$\exp(-5.6120 - 1.1437m - 0.1509m^2)$
$\rho_0(r)$	
Offset	
1 0 0 0	$\exp(-2.4746 - 0.9150m - 0.09179m^2)$
1 1 0 0	$\exp(-4.2383 - 0.9947m - 0.0846m^2)$
1 1 1 0	$\exp(-5.5061 - 0.9809m - 0.1388m^2)$
1 1 1 1	$\exp(-6.6218 - 0.8943m - 0.1969m^2)$

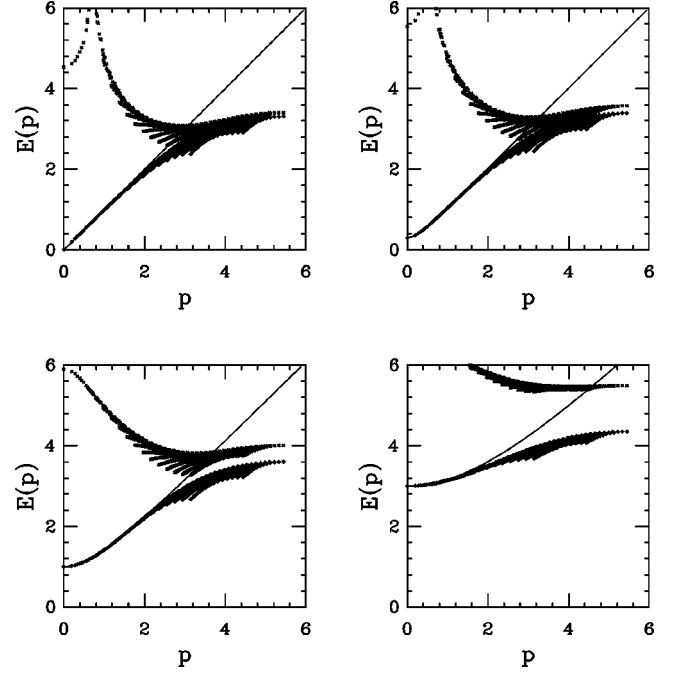


FIG. 10. Dispersion relation for the ‘‘Gaussian’’ hypercubic action, at bare mass (a) zero, (b) 0.3, (c) 1.0, (d) 3.0. The line is the continuum expectation.

APPENDIX: BLOCKING OUT OF THE CONTINUUM

A particularly interesting choice of blocking kernel for blocking out of the continuum is the overlapping transformation

$$\Omega(q) = \exp\left(-\frac{1}{2}c^2q^2\right). \quad (\text{A1})$$

In my work, blocking out of the continuum was approximated by beginning with free Dirac fermions on a fine lattice, making one RG step with a blocking factor $F=8$, and blocking onto a coarse lattice of size 5^4 sites.

Truncating the action to a hypercube and requiring good

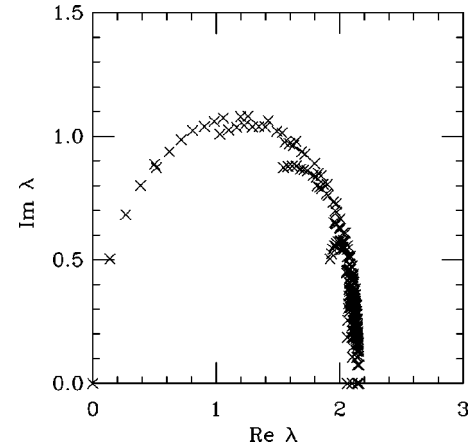


FIG. 11. Eigenmode spectrum of the ‘‘Gaussian’’ hypercubic action.

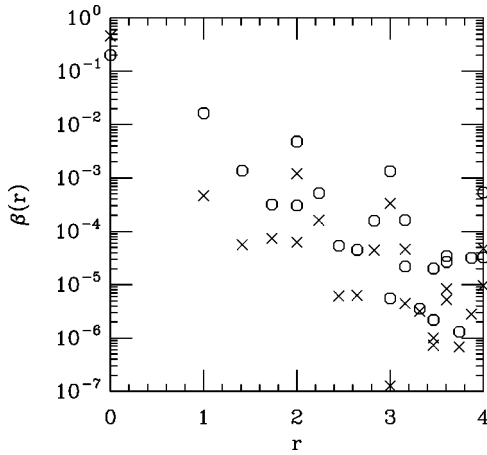


FIG. 12. $\beta(r)$, the scalar part of the free propagator, for the free massless “Gaussian” hypercubic action (crosses) and for the Wilson action (octagons).

behavior for the resulting free hypercubic action leads to the parameter choice $c=0.2$ and $K=2.05$. By beginning with a bare mass m/F on the fine scale I constructed a renormalized trajectory (RT) of free massive fermions. The parametrization and dispersion relation was well behaved out to very large mass ($am \approx 3.0$). The optimum K fell smoothly with increasing m , to a value of 1.0 at $m=3$. This is shown in Fig. 9. In the actual simulations, the hypercubic parameters were

fit to the forms $\rho_j(m)$, $\lambda_j(m) = a \exp(-bm - cm^2)$ and the on-site coupling was fixed using the functional relation between the ρ 's, λ 's, and bare mass m . If negative bare masses are needed, I extrapolated exactly as described in Ref. [1]. The action is listed in Table XI. This is of course not a unique (or probably even an optimal) parametrization.

The free FP field was constructed by summing Eq. (8), in parallel with the FP action. Again, I truncated the FP field to a hypercube and parametrized the “offset” terms exactly as for the hypercubic action. These couplings are shown in Table XII. Both the action and FP field are made gauge invariant by averaging the gauge connections over all the shortest paths, exactly as in Ref. [1].

I show a few properties of the free field action: Figure 10 shows dispersion relations of the hypercubic action on a large lattice, for several values of the bare mass. In Fig. 11, I show the eigenmode spectrum of the hypercubic Gaussian action (with only the positive imaginary part of the complex eigenmodes). The eigenmodes of the FP action lie on a circle of radius $K/2$ centered at the point $(K/2, 0)$, and the approximate action tracks the circle closely. Finally, in Fig. 12, I display the scalar part of the free fermion propagator, $\Delta(r)^{-1} = \beta(r) + i\gamma_\mu \alpha_\mu(r)$. The Ginsparg-Wilson relation for the propagator probes $1/2\{\gamma_5, \Delta(r)^{-1}\} = \gamma_5 \beta(r)$. This is shown for massless fermions on an 11^4 lattice with antiperiodic boundary conditions. For the real FP action, $\beta(r)$ should be proportional to a delta function at the origin. For the hypercubic action it lies about 1–2 orders of magnitude below the value of the Wilson action at all nonzero r .

- [1] T. DeGrand, Phys. Rev. D **58**, 094503 (1998).
[2] T. DeGrand, A. Hasenfratz, and T. Kovacs, Nucl. Phys. **B547**, 259 (1999).
[3] For studies of the Schwinger model, see C.B. Lang and T.K. Pany, Nucl. Phys. **B513**, 645 (1998); F. Farchioni and V. Laliena, in *Lattice '97* [Nucl. Phys. B (Proc. Suppl.) **63**, 907 (1998)]; F. Farchioni, I. Hip, C. Lang, and M. Wohlgenant, in *Lattice '98*, Nucl. Phys. B (Proc. Suppl.) **73**, 939 (1999); hep-lat/9812018; Nucl. Phys. **B549**, 364 (1999); F. Farchioni, I. Hip, and C.B. Lang, Phys. Lett. B **443**, 214 (1998); W. Bietenholz and I. Hip, hep-lat/9902019.
[4] P. Hasenfratz and F. Niedermayer, Nucl. Phys. **B414**, 785 (1994).
[5] U.J. Wiese, Phys. Lett. B **315**, 417 (1993).
[6] W. Bietenholz and U.J. Wiese, Nucl. Phys. **B464**, 319 (1996).
[7] T. DeGrand, A. Hasenfratz, P. Hasenfratz, P. Kunszt, and F. Niedermayer, Nucl. Phys. B (Proc. Suppl.) **53**, 942 (1997).
[8] W. Bietenholz *et al.*, Nucl. Phys. B (Proc. Suppl.) **53**, 921 (1997).
[9] K. Originos *et al.*, in *Lattice '97* [Nucl. Phys. B (Proc. Suppl.) **63**, 904 (1998)].
[10] P. Ginsparg and K. Wilson, Phys. Rev. D **25**, 2649 (1982).
[11] P. Hasenfratz, Nucl. Phys. **B525**, 401 (1998).
[12] P. Hasenfratz, V. Laliena, and F. Niedermayer, Phys. Lett. B **427**, 125 (1998).
[13] M. Lüscher, Phys. Lett. B **428**, 342 (1998).
[14] M. Falcioni, M. Paciello, G. Parisi, and B. Taglienti, Nucl. Phys. **B251** [FS13], 624 (1985); M. Albanese *et al.*, Phys. Lett. B **192**, 163 (1987).
[15] T. DeGrand, A. Hasenfratz, P. Hasenfratz, and F. Niedermayer, Nucl. Phys. **B454**, 587 (1995); **B454**, 615 (1995).
[16] P. Kunszt, Nucl. Phys. **B516**, 402 (1998).
[17] G. Heatlie *et al.*, Nucl. Phys. **B352**, 266 (1991).
[18] M. Bochicchio *et al.*, Nucl. Phys. **B262**, 331 (1985); L. Karsten and J. Smit, *ibid.* **B183**, 103 (1981).
[19] H. Neuberger, Phys. Lett. B **417**, 141 (1998).
[20] Cf. T. Blum, in *Lattice '98*, Nucl. Phys. B (Proc. Suppl.) **73**, 167 (1999).
[21] W. Bardeen, A. Duncan, E. Eichten, G. Hockney, and H. Thacker, Phys. Rev. D **57**, 1633 (1998); W. Bardeen, A. Duncan, E. Eichten, and H. Thacker, *ibid.* **57**, 3890 (1998).
[22] Cf. R. Mawhinney *et al.*, hep-lat/9811026.
[23] T. DeGrand, A. Hasenfratz, and T. Kovacs, Nucl. Phys. **B505**, 417 (1997).
[24] C. Bernard *et al.*, Nucl. Phys. B (Proc. Suppl.) **53**, 212 (1997).
[25] M. Göckeler *et al.*, Phys. Rev. D **57**, 5562 (1998).
[26] R.G. Edwards, U.M. Heller, and T.R. Klassen, Phys. Rev. Lett. **80**, 3448 (1998).
[27] G. Martinelli, C. Sachrajda, and A. Vladikas, Nucl. Phys. **B358**, 212 (1991).
[28] M. Lüscher, S. Sint, R. Sommer, and H. Wittig, Nucl. Phys.

- B491**, 344 (1997).
- [29] L. Maiani and G. Martinelli, Phys. Lett. B **178**, 285 (1986).
- [30] Cf. H. Neuberger, hep-lat/9803011; R. Edwards, U.M. Heller, and R. Narayanan, Nucl. Phys. **B590**, 457 (1999); P. Hernandez, K. Jansen, and M. Lüscher, hep-lat/9808010; A. Borici, Phys. Lett. B **453**, 46 (1999).
- [31] Cf. K. Orginos and D. Toussaint, in *Lattice '98*, Nucl. Phys. B (Proc. Suppl.) **73**, 909 (1999).